

How to Simulate Billiards and Similar Systems

Boris D. Lubachevsky

bdl@bell-labs.com

Bell Laboratories

600 Mountain Avenue

Murray Hill, New Jersey

Abstract

An N -component continuous-time dynamic system is considered whose components evolve autonomously all the time except for in discrete asynchronous instances of pairwise interactions. Examples include chaotically colliding billiard balls and combat models. A new efficient serial event-driven algorithm is described for simulating such systems. Rather than maintaining and updating the global state of the system, the algorithm tries to examine only essential events, i.e., component interactions. The events are processed in a non-decreasing order of time; new interactions are scheduled on the basis of the examined interactions using preintegrated equations of the evolutions of the components. If the components are distributed uniformly enough in the evolution space, so that this space can be subdivided into small sectors such that only $O(1)$ sectors and $O(1)$ components are in the neighborhood of a sector, then the algorithm spends time $O(\log N)$ for processing an event which is the asymptotical minimum. The algorithm uses a simple strategy for handling data: only two states are maintained for each simulated component. Fast data access in this strategy assures the practical efficiency of the algorithm. It works noticeably faster than other algorithms proposed for this model.

Key phrases:

collision detection, dense packing, molecular dynamics, hard spheres, granular flow

1. Introduction

Many continuous time dynamic systems can be accurately approximated by models whose components evolve autonomously all the time except for in discrete asynchronous instances of pairwise interactions. A typical example is a set of chaotically colliding billiard balls. Each ball moves along a straight line until it collides with another ball or an immobile

obstacle. Only pairwise ball collisions are considered, since the probability is zero that more than two balls are involved in the same collision.

Such “billiards” or “hard sphere” models have been in use among computational physicists since the pioneering work [1]. Recently these models have attracted the attention of simulationists [5]. The task of simulation of such a model is reconstruction of the history of each component. Many models, even as far from billiards as models of combat [11], are conceptually similar to billiards. The similarity is in the techniques for handling spatial combinatorics of multitude of asynchronous pairwise interactions. Processing an interaction (two-ball collision) or an autonomous evolution of a component (moving a billiard ball along a straight line) depends on the specific model in hand.

Most of the recent attention has been drawn to the parallelization of such a simulation [5], [8]. However, it remains not obvious how to write a practically efficient serial algorithm for the billiard-type simulation. A “naive” serial algorithm advances the global state of the billiards from collision to collision. The states of all N balls are examined and updated at times $t_0 \leq t_1 \leq t_2 \leq \dots$, where t_0 is the initialization time and t_{i+1} is the nearest next collision time seen at time t_i . The naive scheme is inefficient for large N because of high costs it incurs while performing the following actions:

- (a) the same collision is repeatedly scheduled an order of N times until it occurs,
- (b) at a typical cycle, most balls are not participating in collisions; still, they are examined by the algorithm.

Aside from costly actions (a) and (b), there exists problem (c) of finding an inexpensive method of determining the nearest collision for a chosen ball. A straight-forward method is to compare the chosen ball with $N - 1$ others. The standard improvement in this method is the division of the pool table into an order of N sectors. Only balls in the neighboring sectors have to be checked to determine the immediate collision which reduces the work from $O(N)$ to $O(1)$ per one collision scheduled.

A natural idea for improvement in (a) and (b) is to postpone examining and updating the state of a ball until its collision. Implementing this idea does not appear as easy as it might seem. As the simulation progresses, a scheduled collision of a given ball may require rescheduling. The need for such rescheduling and the desire not to loose information about already planned collisions lead in [1] to a complicated data structure and update scheme called “time-table” in [3]. Observe that, with all its computing inefficiency, the naive scheme has an attractively simple double-buffering data structure. The structure consists of only two copies of the global state vector, the old and the new, so that the new vector is computed on the basis of the old one and, in turn, becomes the old one during the next cycle.

We propose a new serial algorithm for the simulations like billiards. The attraction of this algorithm is that it utilizes a simple and easy to handle double-buffering data structure, while avoiding costly actions (a) and (b). Problem (c) is handled in our algorithm using the standard technique of sectoring. In most cases the algorithm examines and processes only the events whose processing is unavoidable, e.g., ball collisions and boundary crossings. Sometimes, like the naive algorithm, it also processes events whose examining is not necessary. However, the fraction of such overhead events is less than 15% in most experiments, and does not grow with N , while the speed-up due to simplicity of data handling is substantial. The proposed algorithm achieves the same theoretical optimal performances

as other published algorithms, i.e., $O(\log N)$ instructions per one processed event with sectoring and $O(N)$ without. But its practical algorithmic (i.e., computer independent) speed for the billiard case is at least an order of magnitude higher than that of other algorithms. We were able to handle thousands balls and millions of collisions on a non-supercomputer VAX8550 using FORTRAN (using languages better adapted for the computer should result in additional speed-ups). Figure 9.2 in Section 9 represents results of the experiments for 2000 balls. Using the same program on the same computer, the number could be easily increased to 10^4 .

When writing this algorithm we paid special attention to an often overlooked tradeoff between the complexity of data organization and the amount of computations the algorithm is willing to abandon risking to incur them again. For example, to determine the next collision for a ball A we have to try to collide it with any other ball (within its neighborhood, in the presence of sectoring) and then choose the collision closest in time, say it is a collision with ball B . However this collision of A and B may not necessarily be the one which would take place because the tentative partner B , in its turn, may choose an even better party C , $C \neq A$. As a result, later in the computations, A might figure out that the party $B1$, which was previously rated second to best, is to be considered the best.

Rating potential candidates costs computations: the algorithm tries to simulate a potential collision of ball A with a candidate X in order to rate this X . Should the algorithm retain the results of these preliminary simulations which correspond to the second, third etc. to best parties $B1, B2, \dots$ when the best candidate B is being chosen ? Or is it more economical to abandon the information obtained during the rating and, if later needed, simulate these collisions again ? The answer determines the data organization strategy which crucially affects algorithm efficiency. In the billiard case, a "pack rat" strategy entailing a search through dumped items to find the needed one incurs too high a cost. In a general case, the best tradeoff depends on the relative cost of the basic operations, e.g., the amount of computing needed for repeated scheduling versus that needed to retrieve the same data.

Another scale of strategies and the associated tradeoff is that of the "aggressiveness" of precomputation. In a more aggressive strategy, when the next collision for ball A is being scheduled, not only the existing states of other balls are taken into account but also their possible future states which might result from their as yet unprocessed collisions. The degree of aggressiveness might be measured in how many future collisions the other balls are being looked ahead. The two scales are not independent: a more aggressive precomputation requires a more complicated data structure and encourages the choice of a more "pack rat" data handling strategy.

In the described two tradeoff scales, the strategy used in the proposed algorithm is close to the "wasteful" and "lazy" ends of the scales, the opposite of the "pack rat" and "aggressive" ones. Both the storage of not immediately needed data and precomputation lookahead are reduced. The candidates for the next collision for a particular ball which are rated below the winner are abandoned after the winner is chosen. The future collision of a ball is predicted based only on the existing states of the other balls, not on their future states after possible future collisions.

For a reader who is not familiar with simulation terminology, it is worth adding that the proposed is an *event-driven* simulation algorithm in which the state of the simulated

system is examined by the computer only at the times of the *events*, e.g., ball collisions. A computational physicist may be more familiar with the *time-driven* simulation algorithms. Such algorithms (see, e.g., [6]) are usually employed in the many-body problems in which the components, say particles, rather than evolving almost always autonomously, are continuously interacting by exerting short and/or long range forces. The two computational approaches are radically different and each has its own difficulties.

A time-driven algorithm would maintain the snapshot of the states of all the simulated components at a time t and would advance the time from t to $t + \Delta t$ by modifying all these states. Given the same precision of simulation, Δt should be rather small for billiards. As a result, the time-driven algorithm would be tremendously slower than the proposed event-driven algorithm. Event-driven algorithms are the best (and often the only practical) choice for models where discrete instantaneous events occur asynchronously. In the proposed algorithm, if at time t an event involving ball A is processed, only the state of A is examined and explicitly modified. The states of most other balls need not be known at t and are not examined by the algorithm. In fact, the global state is explicitly known at no time t , except $t = 0$. However, if we wish to know the global state, say, if we wish to know the location of each ball at a particular time t , then additional computations of “projecting” the motions of all balls into time point t are required.

The rest of the paper is organized as follows: In Sections 2 to 6, a definition of the basic operations, the data organization, the formulation of the algorithm with examples of its run, and some comments on the practical experience of its implementation are given. These sections should be sufficient for a reader who wishes to understand and write a simulation algorithm for a billiard-like system. Sections 7 and 8 introduce, explain, and analyze the conditions under which this algorithm works correctly. Section 9 presents an application example for the algorithm: a disk packing problem, Section 10 compares the performance of this algorithm with other published proposals, and Section 11 discusses variants of the billiard simulation and other simulation models like billiards including combat models.

2. Basic operations

Assume that a basic function *interaction_time* is available which, given *state1* of component 1 at *time1* and *state2* of component 2 at *time2*, computes the *time* of the next potential interaction while ignoring the presence of other system components:

$$time \leftarrow interaction_time(state1, time1, state2, time2) \quad (1)$$

where $time \geq \max(time1, time2)$. If *interaction_time* can not find such finite *time*, e.g., when two billiard balls are moving away from each other, we assume that $+\infty$ is returned.

In the billiard simulation, the state of a ball is the pair of vectors $state = (position, velocity)$. If the velocities of the balls are constant between the collisions, and all balls are of the same constant diameter D , then (1) is of the form

$$time \leftarrow \max(time1, time2) + t$$

where

$$t = \begin{cases} (-b - \sqrt{b^2 - ac})/a, & \text{if } b \leq 0 \text{ and } b^2 - ac \geq 0 \\ +\infty, & \text{if } b > 0 \text{ or } b^2 - ac < 0 \end{cases} \quad (2)$$

and

$$\begin{aligned} a &= |\text{velocity2} - \text{velocity1}|^2, \\ b &= \langle \text{position20} - \text{position10}, \text{velocity2} - \text{velocity1} \rangle, \\ c &= |\text{position20} - \text{position10}|^2 - D^2, \\ \text{position10} &= \text{position1} + \text{velocity1}(\max(\text{time1}, \text{time2}) - \text{time1}), \\ \text{position20} &= \text{position2} + \text{velocity2}(\max(\text{time1}, \text{time2}) - \text{time2}), \end{aligned}$$

$|v|$ denotes the length of vector v and $\langle u, v \rangle$ denotes the dot product of vectors u and v . The expression for t in (2) is the least real solution $t = t_-$ of the equation $at^2 + 2bt + c = 0$ which is derived from $|p + vt|^2 = D^2$ where $p = \text{position20} - \text{position10}$ and $v = \text{velocity2} - \text{velocity1}$. The meaning of the latter equation and of both its solutions $t = t_-$ and $t = t_+$ is obvious from Figure 2.1. Note that c may equal 0 in which case $t = t_- = 0$ and $\text{time} = \max(\text{time1}, \text{time2})$. This means that *interaction_time* is applied when one ball is already at the site of the scheduled collision.

Two components 1 and 2 with *state1* and *state2* are said to be *interacting*, if

$$\text{interaction_time}(\text{state1}, \text{time}, \text{state2}, \text{time}) = \text{time} \quad (3)$$

holds for any value of *time*. For example, billiard balls i and j of diameter D each with velocities and positions v_i, p_i and v_j, p_j , respectively, are interacting (i.e., colliding), if

$$|p_j - p_i| = D, \langle v_j - v_i, p_j - p_i \rangle \leq 0 \quad (4)$$

Assume that a basic function *jump* is available which, given *state1* and *state2* of interacting components 1 and 2, computes *new_state1* and *new_state2* of these components immediately after the interaction:

$$(\text{new_state1}, \text{new_state2}) \leftarrow \text{jump}(\text{state1}, \text{state2}) \quad (5)$$

When two billiard balls collide, only their velocities experience jumps, not positions. Assuming the energy and momentum are conserved, the tangential components of the initial velocities are not changed, but the normal coordinates are switched as depicted in Figure 2.2.

A ball bouncing off a boundary of the pool table, in principle, needs not be examined by the algorithm. It may be considered as an ordinary point on the autonomous interval of the trajectory. For example, given positions (x_0, y_0) and the velocity vector v of a ball at time $t = 0$, we can construct functions $X(v, x_0, y_0, t)$ and $Y(v, x_0, y_0, t)$ which would return the position $x = X$ and $y = Y$ of the ball at time t without explicitly processing intermediate boundary reflections. The complexity of computations by functions $X()$ and $Y()$ would not depend on the number of bouncing.

In most applications, however, such elaboration would be of little practical use, because the ball would usually collide with another ball after at most one boundary reflection. Besides, an explicit examination of the reflection event might be needed anyway for statistical

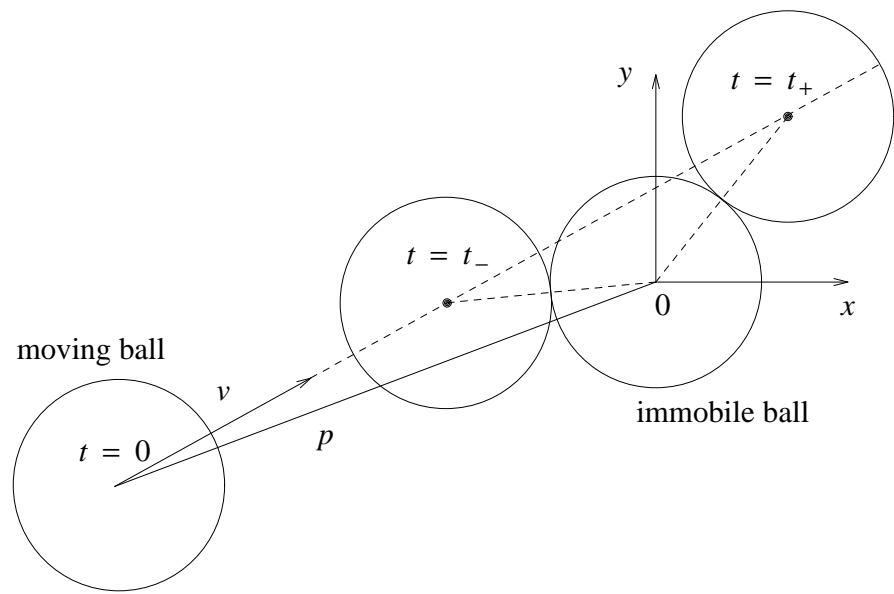


Figure 2.1: The geometrical meaning of the two solutions of equation $|p + vt|^2 = D^2$

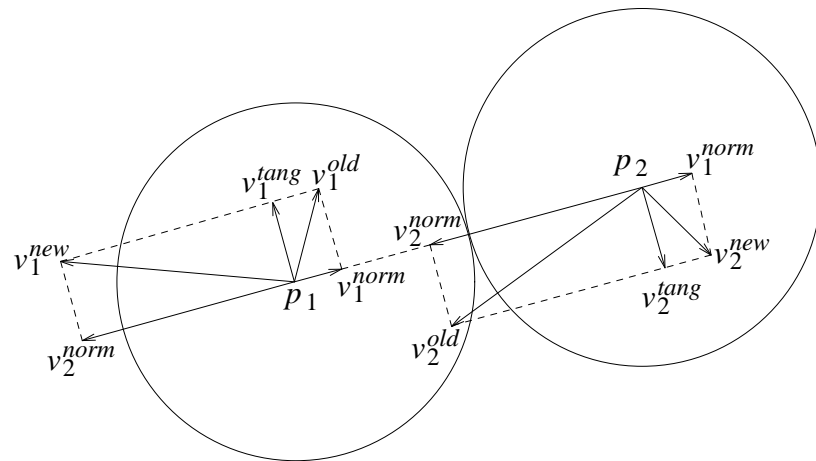


Figure 2.2: Change of velocities of two billiard balls at their collision

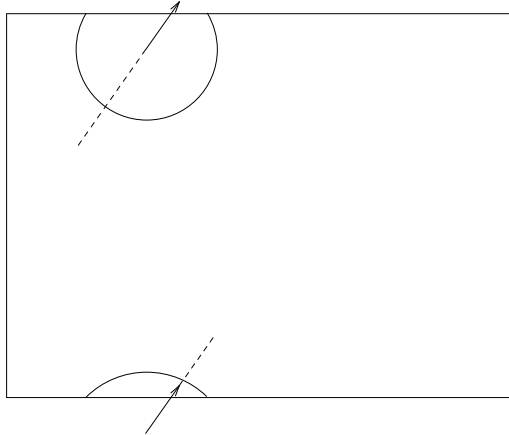


Figure 2.3: A ball is disappearing at a boundary and reappearing at the opposite side under periodic boundary conditions

purposes and for convenience of data update. Thus we will treat a reflection from an immobile obstacle as a separate event.

A boundary crossing may be considered under a periodic boundary condition model, wherein a ball, rather than bouncing off, disappears at a boundary and reappears at the opposite side (see Figure 2.3). This may be treated as the same type of event as boundary reflection. If the pool table is divided into sectors, a similar type of event constitutes a ball moving from one sector to another. Such an event should be examined by the algorithm in order to update the membership in the sectors. We will treat all such events as one-component interactions.

We will assume that basic functions with the same names *interaction_time* and *jump* represent one-component interactions

$$time \leftarrow interaction_time(state1, time1, obstacle) \quad (6)$$

$$new_state \leftarrow jump(state, obstacle) \quad (7)$$

where *obstacle* is the identification of a boundary or an immobile obstacle or a demarcation line. To apply *jump* in (7), the component, whose *state* is represented in (7), must be *interacting* with *obstacle*. The condition which defines such one-component interaction is:

$$interaction_time(state1, time, obstacle) = time \quad (8)$$

holds for any *time*. This is similar to (3). Capital *K* will be reserved for the number of obstacles so that *obstacle* in (6), (7), and (8) is an integer in the interval from 1 to *K*. The one-component versions of functions *interaction_time* and *jump* will be easily distinguished by context from their two-component synonyms in (1) and (3).

We also assume the availability of a basic function *advance* which, given *state0* of a component at *time0* and a value *time1* \geq *time0*, returns *state1* this component would have

at $time1$ ignoring possible interactions with other components or obstacles on the interval $(time0, time1)$:

$$state1 \leftarrow advance(state0, time0, time1) \quad (9)$$

In a frictionless billiard, (9) is of the form

$$\begin{aligned} position1 &\leftarrow position0 + (time1 - time0)velocity0 \\ velocity1 &\leftarrow velocity0 \end{aligned} \quad (10)$$

which simply says that the ball moves with $velocity0$ along a straight line starting from $position0$ at $time0$.

Note that in particular cases, specific calculations for *interaction_time*, *advance*, and *jump* may be not as simple as in the billiard case. The assumption that they are *basic* saves us from the burden to detail them in the general discussion.

3. Data organization

The basic data unit of the algorithm is called *event* and has the following format

$$event = (time, state, partner) \quad (11)$$

where:

time is the time to which *state* of a component corresponds. Note that *state* is the new state of the component *immediately after* the event, e.g., if a ball has experienced a collision at *time*, the velocity-coordinate of the *state* is the new velocity vector after the collision;

partner identifies the other component, if any, involved in the event. If there is no partner in the event, the program assigns a special “no-value” symbol Λ to the *partner* coordinate.

If $time = +\infty$, then the other three coordinates in the *event* have no value, i.e., $state = type = partner = \Lambda$.

At any stage of simulation, the algorithm maintains two events for each component: an old, already processed in the past event and a new, next scheduled event. This information is stored in array $event[1 : N, 1 : 2]$, where N is the number of components of the simulated system. Let us agree to understand a reference like $time[3, 1]$ as the *time* coordinate of element $event[3, 1]$ of this array.

Two arrays $new[1 : N]$ and $old[1 : N]$ with elements equal 1 or 2 are maintained. The value $new[i]$ is the pointer to the new event for component i and the value $old[i]$ is the pointer to the old event for component i , so that new event for component i is stored at $event[i, new[i]]$ and old event for component i is stored at $event[i, old[i]]$. When $new[i]$ is updated, $old[i]$ is updated immediately after, so that relation $new[i] + old[i] = 3$ remains invariant.

4. The algorithm

In the algorithm pseudocode in Figure 4.1, */** and **/* mark the beginning and the end of a comment, the minimum over an empty set of values is assumed $+\infty$, and the following

short-hand notations are used:

$$P_{ij} \stackrel{\text{def}}{=} \text{interaction_time}(\text{state}[i, \text{old}[i]], \text{time}[i, \text{old}[i]], \text{state}[j, \text{old}[j]], \text{time}[j, \text{old}[j]]).$$

where $1 \leq i, j \leq N$ and

$$Q_{ik} \stackrel{\text{def}}{=} \text{interaction_time}(\text{state}[i, \text{old}[i]], \text{time}[i, \text{old}[i]], k)$$

where $1 \leq i \leq N$ and $1 \leq k \leq K$.

The main cycle in Figure 4.1 essentially consists of two steps:

- 1) selecting the next component i_* to process its event (line 2),
- 2) processing the event (the rest of the cycle).

Processing of the event comprises scheduling of the next events for the chosen component and for the other components involved, if any. \mathbf{P} and \mathbf{Q} are the nearest next interaction times. There are two main cases in such scheduling depending on the type of the future event:

- a) when $\mathbf{Q} < \mathbf{P}$, scheduling an interaction which involves only the chosen component i_* (lines 8, 10, and 11);
- b) when $\mathbf{Q} \geq \mathbf{P}$, scheduling an interaction which involves also a second party j_* (lines 8 and 13 - 17) and may involve a third party m_* , the previous partner, if any, of j_* (lines 19 and 20).

Section 5 further explains this simple algorithmic structure in concrete examples of its execution. Now we discuss the aspects of the algorithm which are *not* represented in the aggregated pseudocode in Figure 4.1, namely, the ways the three minimizations in lines 2, 4, and 5 are implemented. Since these techniques are well-known, their discussion will be brief.

Note that for a small number of balls, say $N = 10$, the best way to minimize is to use the straight-forward element-by-element testing. Such straight-forward method to find the minimum of $\text{time}[i, \text{new}[i]]$ for i ranging from 1 to N in line 2 requires $O(N)$ operations per event. Instead, the algorithm organizes values $\text{time}[i, \text{new}[i]]$ into an implicit *heap* structure with two pointer arrays $pht[1 : N]$ and $pth[1 : N]$ so that $\text{time}[pht[m], \text{new}[pht[m]]]$ is the value which is implicitly located at the m -th position of the imaginary heap array and pth is the inverse map for pht , i.e., $pth[pht[m]] = m$ for all m . In particular, $\text{time}[pht[1], \text{new}[pht[1]]]$ corresponds to the heap tree root, i.e., the minimum value. Thus line 2 could be simply rewritten as

$$i_* \leftarrow pht[1], \quad \text{current_time} \leftarrow \text{time}[i_*, \text{new}[i_*]]$$

The payment for this computationally cheap method of finding the minimum is the need to update the heap structure, i.e., arrays pht and pth , each time a value of $\text{time}[i, \text{new}[i]]$ is changed in other sections of the algorithm. The total cost of finding the minimum next event time thus runs to as much as $O(\log N)$ operations per one event. For a large N , the cost $O(\log N)$ is still much better than the original cost of $O(N)$.

The main difficulty in the straight-forward method for minimizations in lines 4 and 5 is the need for computing the $N - 1$ values P_{i_*j} in line 4 and the K values Q_{i_*k} in line 5. The opportunity to decrease the $O(N + K)$ complexity burden of these computations depend on the topology of the evolution space and the uniformity of the component and obstacle distribution in this space. In the billiard case the space is just the Euclidean plane and there is an upper bound on the number of balls which can be located in a bounded vicinity of a given ball. To take a computational advantage of this, the simulation space is divided into sectors and only the components or obstacles incident to the neighboring sectors are examined. The sector boundaries naturally become additional “obstacles” in this method and their processing constitute the method’s overhead. However the practical gain in the method is high as examples in Section 5 and 9 show. Theoretically, the cost reduces to $O(1)$ when using this method.

Among the available grids used for planar sectorization, the grid of equal squares is the most convenient. (The ratio of the area to the perimeter of a sector is larger for the hexagonal grid, though.) Specifically in the case of equal balls, we usually choose square sides larger than the ball diameter, and for each square we maintain the membership linked-list of balls whose centers project to this square. Processing of a square boundary crossing is accompanied by the update of the two lists. Only those P_{i_*j} are computed and are subject to minimization in line 4, for which the center of ball j belongs to one of the nine sectors neighboring the one whose member is i_* .

5. Simple example

Two examples of the execution of the algorithm in Figure 4.1 are reproduced in Figures 5.2 and 5.3. Four-ball billiards are simulated in both examples. The pool table is a square. Unlike real billiards with hard wall boundaries, periodic boundary conditions are assumed (these conditions are explained in Section 2, see Figure 2.3). In the example shown in Figure 5.2, the table is subdivided into 3×3 equal square sectors. Figure 5.2 consists of three frames, a, b, and c. Each frame shows a snapshot of the simulation state at a particular *current_time* with the identification, position, and velocity vector of each ball at this time. Since the execution state usually does not contain positions of all the balls at the same *current_time*, a picture-producing routine (not presented in this discussion) accepts $t = \text{current_time}$ as an input and interpolates between the *old* and the *new* positions of the ball as shown in Figure 5.1. Note that while Figure 5.1 shows a “general” case, with $\text{time}[i, \text{old}[i]] < t < \text{time}[i, \text{new}[i]]$, the snapshots in Figure 5.2 and 5.3 have many “degenerated” cases, e.g., $\text{time}[i, \text{old}[i]] = t$. Also note that for simplicity of the pictures, the times are rounded off to their integer parts (the computer manipulates them with the machine precision for representing real numbers).

Figure 5.2a shows the positions and velocities of the four balls at *current_time* = 0. These quantities are the initial values. Observe that no two balls overlap. (A method to define such initial positions is discussed in Section 9. Correct simulation should preserve this property.) As the initialization statement in Figure 4.1 reads, the balls are initialized at the same zero *time* with identical *old* and *new* events. Succeeding the test in line 1, Figure 4.1

initially $current_time \leftarrow 0$ and for $i = 1, 2, \dots, N$: $new[i] \leftarrow 1$, $old[i] \leftarrow 2$, $time[i, 1] \leftarrow 0$, $partner[i, 1] \leftarrow \Lambda$, $state[i, 1] \leftarrow$ initial state of component i , $event[i, 2] \leftarrow event[i, 1]$

1. while $current_time < end_time$ do {
2. $current_time \leftarrow \min_{1 \leq i \leq N} time[i, new[i]]$;
 $i_* \leftarrow$ an index which supplies this minimum (i.e., $current_time$) ;
3. $new[i_*] \leftarrow old[i_*]$; $old[i_*] \leftarrow 3 - new[i_*]$;
4. $\mathbf{P} \leftarrow \min_{j \in A(i_*)} P_{i_* j}$, where $A(i_*) = \{1 \leq j \leq N, j \neq i_*, time[j, new[j]] \geq P_{i_* j}\}$;
 if $\mathbf{P} < +\infty$ then $j_* \leftarrow$ an index which supplies this minimum (i.e., \mathbf{P}) ;
5. $\mathbf{Q} \leftarrow \min_{k \in B} Q_{i_* k}$, where $B = \{1 \leq k \leq K\}$;
 if $\mathbf{Q} < +\infty$ then $k_* \leftarrow$ an index which supplies this minimum (i.e., \mathbf{Q}) ;
6. $\mathbf{R} \leftarrow \min\{\mathbf{P}, \mathbf{Q}\}$; $time[i_*, new[i_*]] \leftarrow \mathbf{R}$;
7. if $\mathbf{R} < +\infty$ then {
8. $state1 \leftarrow advance(state[i_*, old[i_*]], time[i_*, old[i_*]], \mathbf{R})$;
9. if $\mathbf{Q} < \mathbf{P}$ then {
10. $state[i_*, new[i_*]] \leftarrow jump(state1, k_*)$;
11. $partner[i_*, new[i_*]] \leftarrow \Lambda$;
 } /* end $\mathbf{Q} < \mathbf{P}$ clause */
12. else { /* case $\mathbf{Q} \geq \mathbf{P}$ */
13. $time[j_*, new[j_*]] \leftarrow \mathbf{R}$;
14. $state2 \leftarrow advance(state[j_*, old[j_*]], time[j_*, old[j_*]], \mathbf{R})$;
15. $(state[i_*, new[i_*]], state[j_*, new[j_*]]) \leftarrow jump(state1, state2)$;
16. $m_* \leftarrow partner[j_*, new[j_*]]$;
17. $partner[i_*, new[i_*]] \leftarrow j_*$; $partner[j_*, new[j_*]] \leftarrow i_*$;
18. if $m_* \neq \Lambda$ and $m_* \neq i_*$ then { /* update third party m_* */
19. $state[m_*, new[m_*]] \leftarrow$
 $advance(state[m_*, old[m_*]], time[m_*, old[m_*]], time[m_*, new[m_*]])$;
20. $partner[m_*, new[m_*]] \leftarrow \Lambda$;
 } /* end update third party */
- } /* end $\mathbf{Q} \geq \mathbf{P}$ clause */
- } /* end $\mathbf{R} < +\infty$ clause */
- } /* end while loop */

Figure 4.1: The simulation algorithm

(assuming *end_time* is sufficiently large), the algorithm is searching for a ball index i_* which yields the minimum to $time[i, new[i]]$. As Figure 5.2a indicates, the algorithm has chosen ball 1. Observe that in the beginning of simulation, all four *new* events have the same *time* so the other three choices would be also correct. After switching the senses of *old* and *new* event storages for ball 1 in line 3 (here a redundant manipulation), in line 4 the algorithm tries to select the ball with which ball 1 will collide first. Since $time[i, new[i]] = 0$ for all i and all $P_{ij} > 0$, no j satisfies $time[j, new[j]] \geq P_{i_*j}$. This means that the set subject to minimization in line 4 is empty. Hence $\mathbf{P} = +\infty$, and no j_* is selected. In line 5 the algorithm selects the boundary k_* which will be reached by ball 1 first. This boundary happens to be the lower side of the sector to which *position*[1, *old*[1]] belongs and the ball reaches it (in the absence of other balls) at time $\mathbf{Q} = 58$. In line 6, \mathbf{R} and $time[1, new[1]]$ are becoming equal to this time. Tests in line 7 and 9 are succeeding and the rest of cycle 1 is spent on assigning to the *new* coordinates their scheduled values in lines 8, 10, and 11. These new values will be in effect immediately after crossing the specified boundary. Note that if *obstacle* is a demarcation boundary between sectors, then *jump* is defined as an identical function: $jump(state, obstacle) \stackrel{\text{def}}{=} state$. Then the algorithm takes the snapshot of the situation (and this snapshot is shown in Figure 5.2a), after which cycle 2 is started. On the snapshot, ball 1 has a scheduled event at time 58, while the other three balls still have scheduled events at time 0 as indicated.

Cycles 2, 3, and 4 are spent on scheduling the future events with positive times for the remaining three balls. Figure 5.2b shows the progress made in this scheduling. While *current_time* is still at 0 because no event with positive time has been processed yet, balls 2 and 3 have scheduled boundary crossings (case $\mathbf{Q} < \mathbf{P}$) and ball 4 has scheduled a collision at time 25 with ball 1 (case $\mathbf{Q} \geq \mathbf{P}$). When a scheduled collision is indicated on a picture, not only its time is given but also (in parentheses) the partner index. Thus, (4)25 at the *new* position of ball 1 means that (the center of) ball 1 reaches this position at time 25 and when it does so, it collides with ball 4. (The dashed line which is supposed to indicate the future motion of ball 4 is overstricken by the arrow indicating the velocity.)

The algorithm schedules this collision at cycle 3 when balls 1 and 2 have already scheduled their next events, boundary crossings at times 58 and 124 respectively, but ball 3 has not been touched by the algorithm yet. This scheduling proceeds as follows. First (line 4), ball $i_* = 4$ finds out that the only P_{4j} which is not larger than $time[j, new[j]]$ is $P_{41} = 25$ and \mathbf{P} becomes 25. Then (line 5), it is determined that the nearest boundary crossing occurs at time \mathbf{Q} . The smallest of the two, \mathbf{P} and \mathbf{Q} , becomes \mathbf{R} and also $time[4, new[4]]$ in line 6. Since \mathbf{R} is finite and \mathbf{Q} is larger than \mathbf{P} , test in line 7 succeeds but test in line 9 fails. As a result, the sequence of statements in lines 8 and 13 - 17 is executed whereby balls 4 and 1 have scheduled a collision at time 25 and the index m_* of the third party is remembered. Since there was no partner in the previously scheduled by ball 1 *new* event, m_* becomes Λ and lines 19 and 20 are skipped.

Time 25 becomes the smallest one in the event-list and the next two cycles, 5 and 6, are spent on processing two events, *event*[1, *new*[1]] and *event*[4, *new*[4]], both representing the collision of balls 1 and 4 at time 25 but from the “viewpoints” of two different balls. Processing the collision event by ball 1 generates new boundary crossing scheduled for time

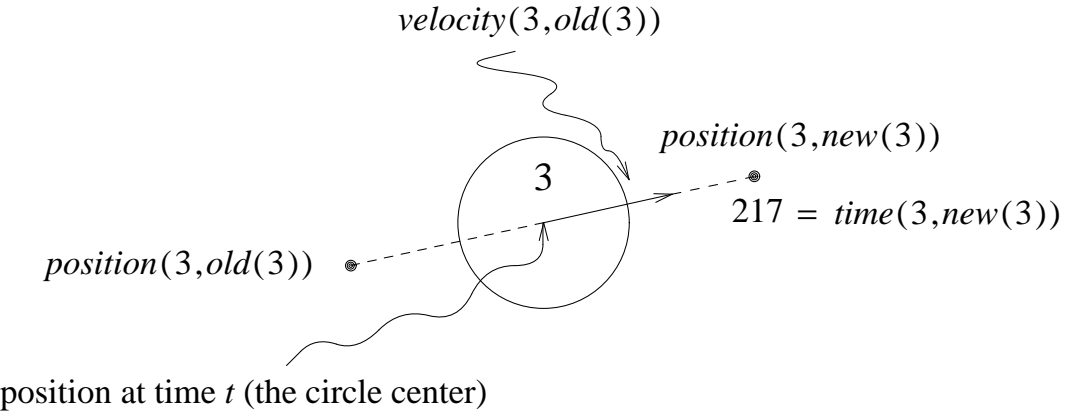


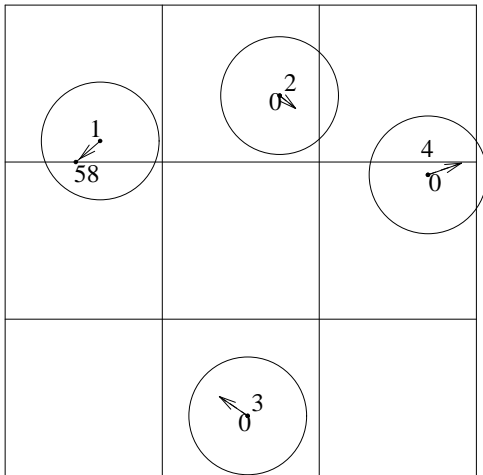
Figure 5.1: Ball 3 at time $current_time = t$ (a legend for Figure 5.2 and 5.3)

94 and processing the collision by ball 4 generates another collision scheduled for time 87 with ball 2. The latter collision preempts the previously scheduled by ball 2 boundary crossing for time 124. The result of all these processings is shown in Figure 5.2c. Two velocity vectors are indicated for each colliding ball in Figure 5.2c: before and after the collision. As seen, ball 1 has collided not with ball 4 but with its periodic image.

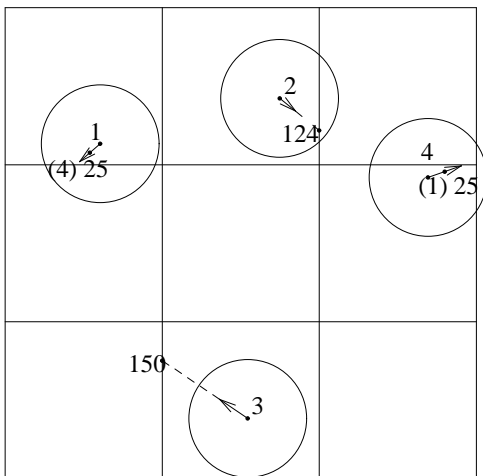
The sequence of snapshots shown in Figure 5.3 corresponds to the same initial condition of the balls as in Figure 5.2 but without sectoring. During cycles 1 to 4 two collisions are scheduled: one of balls 1 and 4 for time 25 and another of balls 2 and 3 for a distant time 388. However after cycle 5 the more distant collision of balls 2 and 3 is preempted by a collision of balls 1 and 2 for earlier time 226. As a result, ball 3 is left without a collision; its tentative collision is turned into a no-partner event which will be convenient to call *advancement*. However, at cycle 6 the preemptor, collision of balls 1 and 2 for time 226, is itself preempted by a collision of balls 2 and 4 scheduled for even earlier time 87. As a result, ball 1 has now scheduled an advancement event, the one previously believed to be a collision scheduled for time 226.

It seems that events develop faster in the experiments without sectoring shown in Figure 5.3 than in those with sectoring in Figure 5.2. Without sectoring the balls attempt to schedule their new events with larger horizons, they are more “aggressive.” However, each cycle here takes more computing time. We have continued both experiments for 10^5 collisions, each pairwise collision counted twice. Without sectoring, it takes more than three times longer of the CPU time, than with sectoring.

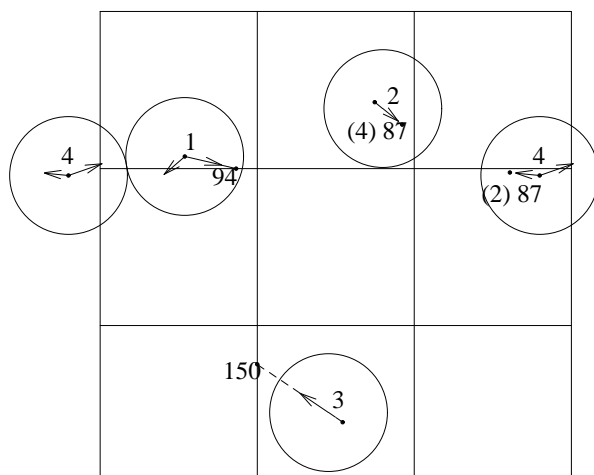
This is so because to schedule a collision with sectoring, a ball should check nine neighboring sectors including its own, where it finds at most three other balls. Without sectoring a ball should check the same three balls, and also their 3×8 periodic boundary images. Functions *interaction_time* are formally different in the two cases. In the case without sectors, time of a next collision with a ball A is in fact given not as (2) but as the minimum of nine times, one of which represents a collision with A and is given by (2) and the other eight represent collisions with eight periodic images of A .



a) result of cycle 1; $current_time = 0$; ball 1 has scheduled a boundary crossing for time 58

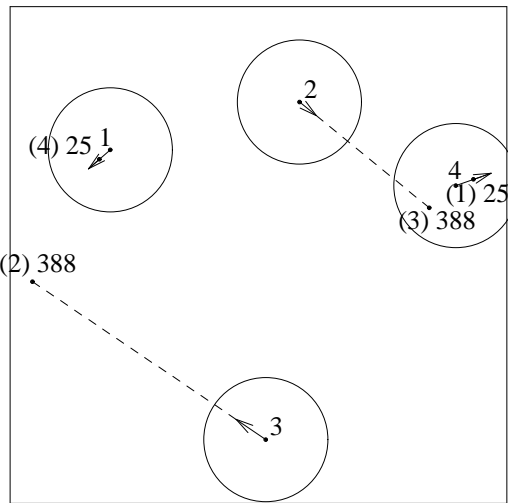


b) result of cycles 2, 3, and 4; $current_time = 0$; ball 2 has scheduled a boundary crossings for time 124; ball 3 has scheduled a boundary crossing for time 150; ball 4 has scheduled a collision with ball 1 for time 25

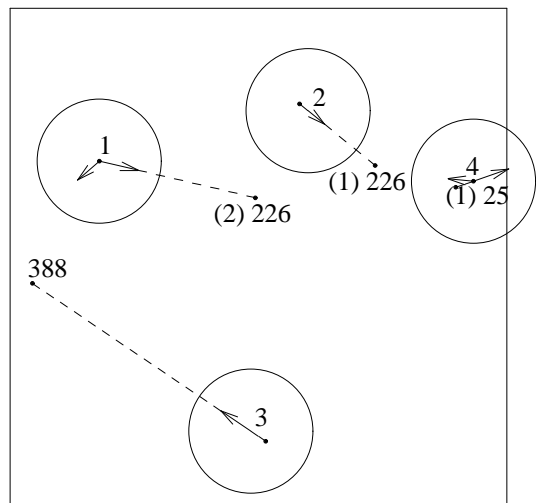


c) result of cycles 5 and 6; $current_time = 25$; balls 1 and 4 have processed a collision for time 25; ball 1 has scheduled a boundary crossing for time 94; balls 2 and 4 have scheduled a collision for time 87

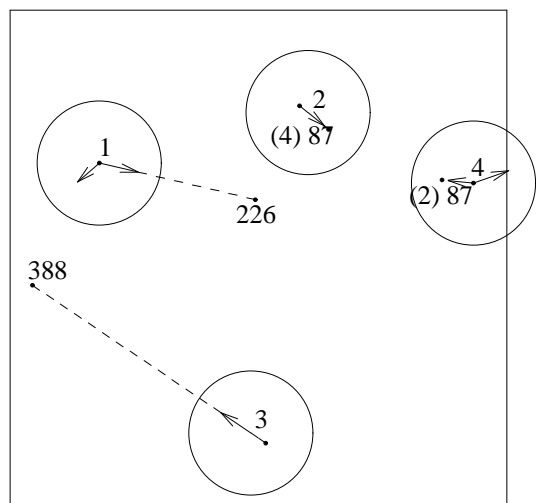
Figure 5.2: An example of the algorithm execution. Space is sectorized



a) result of cycles 1 to 4; $current_time = 0$; balls 1 and 4 have scheduled a collision for time 25; balls 2 and 3 have scheduled a collision for time 388



b) result of cycle 5; $current_time = 25$; ball 1 has processed its collision with ball 4 for time 25; balls 1 and 2 have scheduled a collision for time 226; ball 2 canceled an earlier scheduled collision with ball 3 for later time 388 and this collision is turned into an advancement for ball 3



c) result of cycle 6; $current_time = 25$; ball 4 has processed its collision with ball 1 at time 25; balls 2 and 4 have scheduled a collision for time 87; ball 2 has canceled an earlier scheduled collision with ball 1 for later time 226 and this collision is turned into an advancement for ball 1

Figure 5.3: An example of the algorithm execution. Space is not sectorized. The initial conditions for the balls are the same as in Figure 5.2

6. Comments on the practical execution of the algorithm

Overlaps. A practically working algorithm for billiard simulation should be resistant with respect to small overlap of the balls. Figure 5.3 shows “a preemption of a preemptor” phenomenon when ball 1 has preempted a collision of balls 2 and 3 by scheduling an earlier collision with ball 2 (Figure 5.3b) only to be later preempted by ball 4 which schedules an even earlier collision with ball 2 (Figure 5.3c). In the simulations with thousands of balls, more involved phenomena of this kind occur. Combined with the roundoff, occasionally, they cause small overlaps of the balls as shown in the following example. Suppose, a scheduled collision of balls A and B for time t_{AB} is later preempted by scheduling collision of B and C for time $t_{BC} < t_{AB}$. As a result, the collision event for A becomes an advancement for time t_{AB} . Suppose, that later, collision of C and D scheduled for time $t_{CD} < t_{BC}$ preempts the collision of B and C . As a result, the collision event for B becomes an advancement for time t_{BC} . Now the originally scheduled collision of A and B for time t_{AB} needs to be scheduled again. However, it will be done starting with different initial positions. If formula (2) is used in this scheduling, then $c = 0$ and $t = 0$ because $\max(\text{time1}, \text{time2}) = t_{AB}$. Because of roundoff errors and different computational paths, c may be “slightly” negative as if balls A and B would slightly overlap at time t_{AB} and so negative could be t . In the existing program this problem is handled as follows: whenever *interaction_time* computes a negative but small by absolute value t in (2), this is not reported as an error, but the value of t is replaced by zero.

Advancement events. A preempted two-component interaction is turned into an advancement for the third party, e.g., the preempted collision for time 388 of balls 2 and 3 in Figure 5.3a is turned for ball 3 into an advancement in Figure 5.3b. A more aggressive strategy would perform a full-fledged new event scheduling for ball 3. Such strategy is less efficient partly because advancements are usually far fetched in the future and have a great chance to be rescheduled so it is not worthwhile to waste precomputations on them. By the time of event processing only a small fraction of events remain advancements, in most simulated cases less than 15%. More importantly, the fraction of the processed advancements does not grow with N . (No theoretical analysis of this statement is available.) Another possibility is “rolling back” the preempted ball to the *old* event. This would break the time-orderly event processing.

Delayed update. There exists a subtle inefficiency in the algorithm in Figure 4.1. When scheduling an interaction, the algorithm applies *advance* and *jump* operations. If the event is later preempted, these computations are wasted. For example, when scheduling a collision of balls 2 and 3 for time 388 (Figure 5.3a), new velocities are computed, using *jump*. Later, however, this collision is preempted (Figure 5.3b). To correct this inefficiency, the application of *advance* and *jump* should be delayed until the latest possible moment when the scheduled event is being processed. Such optimized pseudocode (which looks less transparent than the original one) is given in Figure 6.1.

The encoding of *partner* is different in the algorithm in Figure 6.1 comparing with that

initially $current_time \leftarrow 0$ and for $i = 1, 2, \dots, N$: $new[i] \leftarrow 1$, $old[i] \leftarrow 2$, $time[i, 1] \leftarrow 0$, $partner[i, 1] \leftarrow \Lambda$, $state[i, 1] \leftarrow$ initial state of component i , $event[i, 2] \leftarrow event[i, 1]$

1. while $current_time < end_time$ do {
2. $current_time \leftarrow \min_{1 \leq i \leq N} time[i, new[i]]$;
 $i_* \leftarrow$ an index which supplies this minimum (i.e., $current_time$) ;
3. $state1 \leftarrow advance(state[i_*, old[i_*]], time[i_*, old[i_*]], time[i_*, new[i_*]])$;
4. $j_\# \leftarrow partner[i_*, new[i_*]]$;
5. if $j_\# = \Lambda$ then $state[i_*, new[i_*]] \leftarrow state1$
6. else /* case $j_\# \neq \Lambda$ */
 if $j_\# > 0$ then /* state update required */
 if $j_\# > N$ then /* one-component interaction */
 $state[i_*, new[i_*]] \leftarrow jump(state1, j_\# - N)$
7. else { /* $1 \leq j_\# \leq N$, two-component interaction */
 $state2 \leftarrow advance(state[j_\#, old[j_\#]], time[j_\#, old[j_\#]], time[j_\#, new[j_\#]])$;
 $(state[i_*, new[i_*]], state[j_\#, new[j_\#]]) \leftarrow jump(state1, state2)$;
 $partner[j_\#, new[j_\#]] \leftarrow -i_*$; /* negative partner flags no state update for $j_\#$ */
 } /* end two-component interaction clause,
 end state update required clause, end $j_\# \neq \Lambda$ clause */
8. $new[i_*] \leftarrow old[i_*]$; $old[i_*] \leftarrow 3 - new[i_*]$;
9. $\mathbf{P} \leftarrow \min_{j \in A(i_*)} P_{i_* j}$, where $A(i_*) = \{1 \leq j \leq N, j \neq i_*, time[j, new[j]] \geq P_{i_* j}\}$;
 if $\mathbf{P} < +\infty$ then $j_* \leftarrow$ an index which supplies this minimum (i.e., \mathbf{P}) ;
10. $\mathbf{Q} \leftarrow \min_{k \in B} Q_{i_* k}$, where $B = \{1 \leq k \leq K\}$;
 if $\mathbf{Q} < +\infty$ then $k_* \leftarrow$ an index which supplies this minimum (i.e., \mathbf{Q}) ;
11. $\mathbf{R} \leftarrow \min\{\mathbf{P}, \mathbf{Q}\}$; $time[i_*, new[i_*]] \leftarrow \mathbf{R}$;
12. if $\mathbf{R} < +\infty$ then
 if $\mathbf{Q} < \mathbf{P}$ then $partner[i_*, new[i_*]] \leftarrow N + k_*$
 else { /* case $\mathbf{Q} \geq \mathbf{P}$ */
 $time[j_*, new[j_*]] \leftarrow \mathbf{R}$;
 $m_* \leftarrow partner[j_*, new[j_*]]$;
 $partner[i_*, new[i_*]] \leftarrow j_*$; $partner[j_*, new[j_*]] \leftarrow i_*$;
 if $m_* \neq \Lambda$ and $m_* \neq i_*$ then $partner[m_*, new[m_*]] \leftarrow \Lambda$;
 } /* end $\mathbf{Q} \geq \mathbf{P}$ clause */
13. } /* end while loop */

Figure 6.1: A version of the simulation algorithm with delayed state update

in Figure 4.1. In the new version,

$$partner[i, new[i]] = \begin{cases} \Lambda & \text{for an advancement} \\ \text{the index of the partner} & \text{for a two-component interaction} \\ N + \text{the index of the obstacle} & \text{for a one-component interaction} \end{cases} \quad (12)$$

assuming the interaction has not been processed yet. After the interaction has been processed by one participant i_* but not by the other j_* , $partner[j_*, new[j_*]]$ becomes negative to indicate that no state update by the second participant j_* is required. This is so done because processing for ball i_* has updated both states.

This code saves not a great deal in the billiard case because here *advance* and *jump* are much lighter computationally than *interaction_time*. The update pattern of array $time[1 : N, 1 : 2]$ in the algorithm in Figure 6.1 is the same as in the one in Figure 4.1.

When the third party is the first party ? In both versions of the algorithm, the third party update is conditioned to $m_* \neq i_*$ (lines 18, 19 and 20 in Figure 4.1 and line 23 in Figure 6.1), which requires the third party to be distinct from the first party, the initiator of the update. The existing program for billiard balls is supposed to report an occurrence of $m_* = i_*$. In all the runs, this condition has never been reported. Is identity $m_* = i_*$ at all possible ?

We can imagine a scenario when equality $m_* = i_*$ is caused by two components interacting twice, second interaction immediately after the first one without intermediate involvement of other components or obstacles. In the billiard case with periodic boundary conditions two subsequent collisions of the same pair of balls is highly improbable for large N . For small N , e.g., $N = 2$, if balls are relatively large, this can occur with a high probability. In other systems such occurrences may be probable even for large N . That is why in the general algorithms, the execution is safeguarded with the test $m_* \neq i_*$.

7. Consistency of basic operations

In the billiards application, the three basic functions of Section 2 are defined in terms of a consistent model: by integrating differential equations of motion of a system, using conservation laws, etc. However, the formulation of the algorithm in Section 4 employs no additional model. Clearly, arbitrarily “bad” basic functions can cause arbitrarily bizarre behavior even of a “good” algorithm. Thus, if we wish to provide certain assurance that the algorithm is “correct,” we should request certain “correctness” or consistency properties of the basic functions. Thus, we introduce the following conditions:

- (I) Function *interaction_time* is commutative with respect to the components, i.e., it depends on the unordered pair of components, although in (1) the two participants in the interaction are represented in a particular order.
- (II) Similarly, function *jump* depends only on the unordered pair of arguments. This means that assignment $(new_state2, new_state1) \leftarrow jump(state2, state1)$ produces the same new_state1 , and new_state2 as assignment (5).

(III) Function $advance(state0, time1, time2)$ satisfies a two-parametrical semigroup property with respect to its second and third argument, i.e., for any $t_1 \leq t_2 \leq t_3$ we have $advance(advance(s, t_1, t_2), t_2, t_3) = advance(s, t_1, t_3)$ for any state s .

(IV) Moreover, there is a proper associativity between $advance$ and $interaction_time$, namely, if $t = interaction_time(s_1, t_1, .)$, and $t_1 \leq t_2 \leq t$, then $t = interaction_time(advance(s_1, t_1, t_2), t_2, .)$, where dot $(.)$ replaces an appropriate pair $(state, time)$ if we have a two-component interaction or it replaces an *obstacle* if we have a one-component interaction. For a two-component $interaction_time$, this property, coupled with (I), implies a similar associativity with respect to the second set of arguments or with respect to both sets.

(V) The components are never stuck at each other. Namely, if two components 1 and 2 with $state1$ and $state2$ are interacting, i.e. (3) holds, *jump* is applied and new_state1 and new_state2 are computed according to (5), then $interaction_time(new_state1, time, new_state2, time) > time$. Similarly, if a component with $state$ is interacting with *obstacle*, i.e. (8) holds, *jump* is applied and new_state is computed according to (7), then $interaction_time(new_state, time, obstacle) > time$.

Computationally conditions (I) - (IV) might be “slightly” violated because of the round-off. This can cause dependence of the simulated history on the processing order. In double-precision billiard simulations, a few dozen collisions experienced by each ball is usually sufficient for two differently ordered computations to completely diverge, even when started with identical initial conditions. After the divergence the ball trajectories and the collisions that occur in one such run are completely different from the trajectories and collisions that occur in the other. Computational physicists are aware of such divergence [3] and consider it a variant of physical irreproducibility. It is worth stating however that the second run of exactly the same serial program starting with the same input data produces exactly the same results.

Now we are going to introduce a condition of a different kind. Consider the set of components and obstacles $I(t)$ interacting at a particular time t . If $I(t)$ is non-empty, we may introduce a binary relation among the elements in $I(t)$, assuming element i is in the relation with element j if i is interacting with j at t . Let \sim be a reflexive, symmetric, and transitive closure of this relation, so that \sim is an equivalence.

With this definition, the condition is:

(VI) No equivalence class for the relation \sim contains more than two elements.

In the billiard case, (VI) prohibits, for example, participation of more than two balls in the same collision (but several disjoint pairwise collisions may take place at the same time). Figure 7.1 shows such prohibited triple collision where (4) holds for the pair $(i = 1, j = 2)$ and, separately, for the pair $(i = 2, j = 3)$, but not for the pair $(i = 1, j = 3)$, because $|p_1 - p_3| > D$.

In Figure 7.1, the initial condition before collision, including positions of the balls and

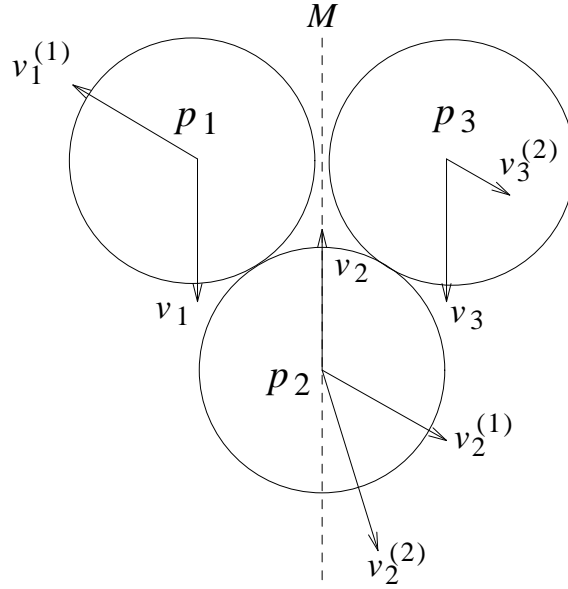


Figure 7.1: A triple collision

their velocities v_1, v_2 and v_3 , is mirror symmetrical with respect to the middle vertical line M . There are two possible orders of processing this collision by the algorithm. In one order, balls 1 and 2 collide first and obtain new velocities $v_1^{(1)}$ and $v_2^{(1)}$, and then balls 2 and 3 collide and obtain new velocities $v_2^{(2)}$ and $v_3^{(2)}$. The initial velocity of ball 2 for the second pairwise collision is $v_2^{(1)}$ as if the second collision occurred later than the first one. The net result of the triple collision is the three balls moving away from the collision site with velocities $v_1^{(1)}, v_2^{(2)}$, and $v_3^{(2)}$, which are not mirror symmetrical with respect to M . Hence, the outcome of the triple collision depends on the order of processing and so the history of the entire simulation.

With infinite precision computations, in the case of chaotically colliding billiard balls, the probability of violating (VI) is zero. However, in our finite precision experiments multiple collisions could practically occur and hence (VI) could be violated. The proof in Section 8 of correctness of the simulated trajectory should be understood as an assurance that if the machine precision is infinite, the correctness holds for as long as (VI) holds.

In order to show that the algorithm in Figure 4.1 reconstructs the trajectory of each component “correctly” we must know what a “correct” trajectory is. With assumptions (I) - (VI), starting with a global state at time 0, we can uniquely define the system state at any positive time using the naive algorithm discussed in Introduction. We *call* the obtained trajectory the correct one.

The algorithm in Figure 4.1 ignores many events on this trajectory. The task of proof is showing that despite of this the trajectory does not change.

8. Invariants and correctness proof

The actions of either simulation algorithms in Figure 4.1 or in Figure 6.1 can be summarized as follows: a repeated update of arrays $new[1 : N]$, $old[1 : N]$, and $event[1 : N, 1 : 2]$ in such a way that the following conditions remain invariant:

$$\max_{1 \leq i \leq N} time[i, old[i]] \leq \min_{1 \leq i \leq N} time[i, new[i]] \quad (13)$$

for $i = 1, 2, \dots, N$ we have:

$$time[i, new[i]] \leq \min \left\{ \min_{1 \leq j \leq N, j \neq i, time[j, new[j]] \geq P_{ij}} P_{ij}, \min_{1 \leq k \leq K} Q_{ik} \right\} \quad (14)$$

and

$$\begin{aligned} & \text{either } partner[i, new[i]] = \Lambda, \\ & \text{or } j = partner[i, new[i]] \text{ is an integer in the interval } N + 1 < j \leq N + K, \\ & \text{or } j \text{ is an integer in the interval } 1 \leq j \leq N \text{ and } partner[j, new[j]] = i \end{aligned} \quad (15)$$

Conditions (13), (14), and (15) are trivially satisfied in the beginning of the simulation. Invariance of condition (13) is obvious. As to (14) and (15), their invariance can be violated temporarily after a cycle during which one component participating in a two-component interaction has been processed but the other has not been yet. After both components have been processed, and no other two-component interaction processing has been started, (14) and (15) hold. For (14), it follows from lines 4, 5, and 6 in Figure 4.1 and for (15), it follows from symmetry of matrix P_{ij} . The symmetry is an obvious implication of (I) and (II). Observe, that invariance of (13) and (14) requires no consistency conditions (I) - (VI).

Invariant (14) is the key to understanding the “wasteful” strategy of the data update in this algorithm. Consider an example. Let $N = 3, K = 0$. Figure 8.1 shows trajectories of three billiard balls A , B , and C . We assume that at time $t = 0$ the balls are positioned on the same horizontal line and we suppose that these are their old positions, i.e., those stored in array $event[., old[.]]$.

On the basis of the old events only, C can see two immediate collisions, one with B when the balls occupy positions $B2$ and $C2$; we call it collision $B2, C2$, and the other with A , namely collision $A2, C1$. C also notes that both A and B have a scheduled event at time earlier than times of either $A2, C1$ and $B2, C2$. Thus, the set of balls X over which the minimum of P_{CX} is to be taken according to (14) is empty and this minimum together with the time of the immediate next interaction for C is $+\infty$.

With the given old events, the following assignment of new times would satisfy (14): both $time[A, new[A]]$ and $time[B, new[B]]$ are equal to the time of collision $A1, B1$, and $time[C, new[C]] = +\infty$. With such an assignment, three inequalities (14) turn into equalities.

The assignment $time[i, new[i]] = +\infty$ simply means that C sees no future interaction at this stage of simulation. A more aggressive strategy of precomputation, in which C would look one more step ahead and would examine possible collisions with A and B based on their velocities after an as yet unprocessed collision $A1, B1$, is possible but is prohibited in the proposed algorithm. Such an aggressive strategy perhaps would work well for a small

number of balls but if there are many of them, it would require a complicated data structure to support an arbitrary-many-step lookahead. Following our “lazy” or “wasteful” strategy, C does not do this and does not schedule for more than one step ahead. This allows us to keep data structure very simple.

Invariants (13) and (14) imply the following useful invariant

$$\min\left\{\min_{1 \leq i, j \leq N} P_{ij}, \min_{1 \leq i \leq N, 1 \leq k \leq K} Q_{ik}\right\} \geq \min_{1 \leq i \leq N} \text{time}[i, \text{new}[i]] \quad (16)$$

Now we prove correctness of the algorithm. The proof proceeds by showing that if

(*) the simulated trajectory is identical to the “correct” one defined in Section 7, for all t in the interval $0 \leq t \leq \max_{1 \leq i \leq N} \text{time}[i, \text{old}[i]]$,

then

(**) after all events with times equal to $\min_{1 \leq i \leq N} \text{time}[i, \text{new}[i]]$ will be processed, the thus extended simulated trajectory will be identical to the “correct” trajectory for all t in the interval $0 \leq t \leq \min_{1 \leq i \leq N} \text{time}[i, \text{new}[i]]$.

This would constitute the inductive step, while the base for the induction is obviously satisfied since (*) is correct for the program state initialized for $t = 0$ as described in Figure 4.1.

The “correct” trajectory has no interaction on the open interval

$$\max_{1 \leq i \leq N} \text{time}[i, \text{old}[i]] < t < \min_{1 \leq i \leq N} \text{time}[i, \text{new}[i]],$$

because if it did, (16) would be violated. Hence the simulated trajectory is identical to the “correct” one for all t in the interval $0 \leq t < \min_{1 \leq i \leq N} \text{time}[i, \text{new}[i]]$. By (I) - (VI), this property extends to the point $t = \min_{1 \leq i \leq N} \text{time}[i, \text{new}[i]]$ and this completes the proof.

9. An application example: disk packing problem

The following model is simulated in [7]: N points are placed randomly within an $L \times L$ square. Periodic boundary conditions apply in both directions. The N points are assigned random initial velocities and in the absence of subsequent collisions would move with these velocities along straight lines threading through an infinite sequence of periodic images of the basic square. However, the points also begin to grow at a common rate into elastic rigid disks, with diameters that are given by linear function of time $D(t) = at$, $t > 0$. As a result, particle collisions become possible, and increase in frequency as $D(t)$ increases. We permit $D(t)$ to grow until the system “jams up” thus obtaining the final packing.

This is a variant of the billiard simulations. Two differences are:

- 1) instead of equation $|p + vt|^2 = D^2$ as in Figure 2.1, equation $|p + vt|^2 = (at)^2$ has to be solved; the latter is still a quadratic equation with respect to t
- 2) the normal components of v_1^{new} and v_2^{new} , the velocities of disks after a collision (see

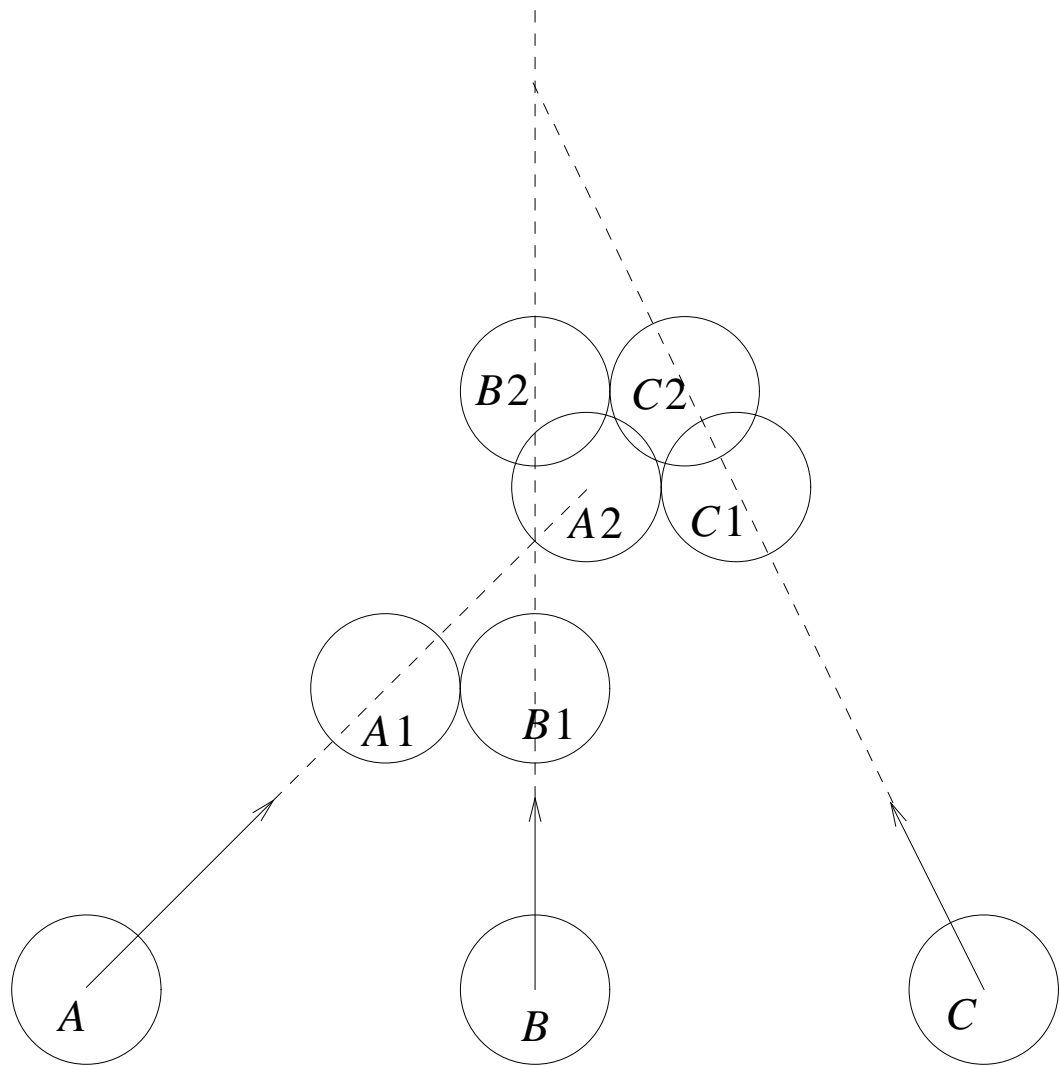


Figure 8.1: Asynchronous collisions of three billiard balls

Figure 2.2), have to be increased to guarantee that disks do not overlap or stick at each other. Any additive velocity larger than $a/2$ would be appropriate.

Energy or momentum conservation are lost with such an additive; as the simulation progresses the system “heats up” and as the disk speeds reach large values computational precision may be lost. The existing program once in a while interrupts the simulation projecting all the disk positions into a particular time value, then scales down and balances them. (The velocities $v_i, i = 1, \dots, N$, of N disks of equal masses are said to be balanced if $\sum_{1 \leq i \leq N} v_i = 0$.)

Figure 9.1 and 9.2 show some results of these experiments, in particular show “rattler” disks which remains unjammed within the walls of jammed neighbors [7]. In the experiment presented in Figure 9.2, the large square is subdivided into 40×40 small square sectors. Rather than checking a possible next collision with 8×1999 candidates, only about 10 disk candidates for the next collision are checked.

10. Comparing practical performance of the algorithm with the other published algorithms

Physicists often study hard-sphere and hard-disk models using computing experiments. However, with the exception of [3] and [1], nobody discusses the details of the algorithms used and with the exception of [1], nobody gives performance data.

We read in [1]: “The IBM704 calculator handles about 2000 collisions per hour for 100 molecules and about 500 collisions per hour for 500 molecules”

Assuming that IBM704 was not slower than 0.02 MFLOP [2] this scales up to no more than 30 collisions per second for a 1 MFLOP machine. The speed of our calculations is in the range 150 - 450 pairwise collisions per second (independently of the number of disks) on VAX8550 which has speed 1 MFLOP. Thus, even the most pessimistic comparison with [1] gives about an order of magnitude speed-up of our algorithm.

Simulation of 50000 to 55000 committed events in a random configuration of 160 disks is reported in [5]. Let us count one pairwise collision as two committed events, and one sector boundary crossing or cushion reflection as one committed event.

The model [5] is different from the one we simulated in that instead of periodic boundary conditions, rigid elastic “cushions” are employed to guard the cell boundaries. To compensate for the difference, let us equate an external boundary crossing in program [7] with one cushion reflection in [5]. Note that when scheduling a collision close to the cell boundary, program [7] considers not only internal disks as the candidates for collision, as program [5] does, but also their periodic images. This additional complexity in program [7] more than compensates for a possible loss of complexity due to substituting a cushion reflection with a boundary crossing.

To make a fair comparison, ratio of the diameter to L must be set as in [5]. Since the value of this ratio is not indicated in [5], different pictures of 160 randomly placed disks for several different diameters were produced and the one which resembled the most Figure 9 in [5] was selected. In the selected picture, the ratio is 0.015. Then we made a measuring run, in which sector boundary crossings were counted only for 16 sectors as specified in series I

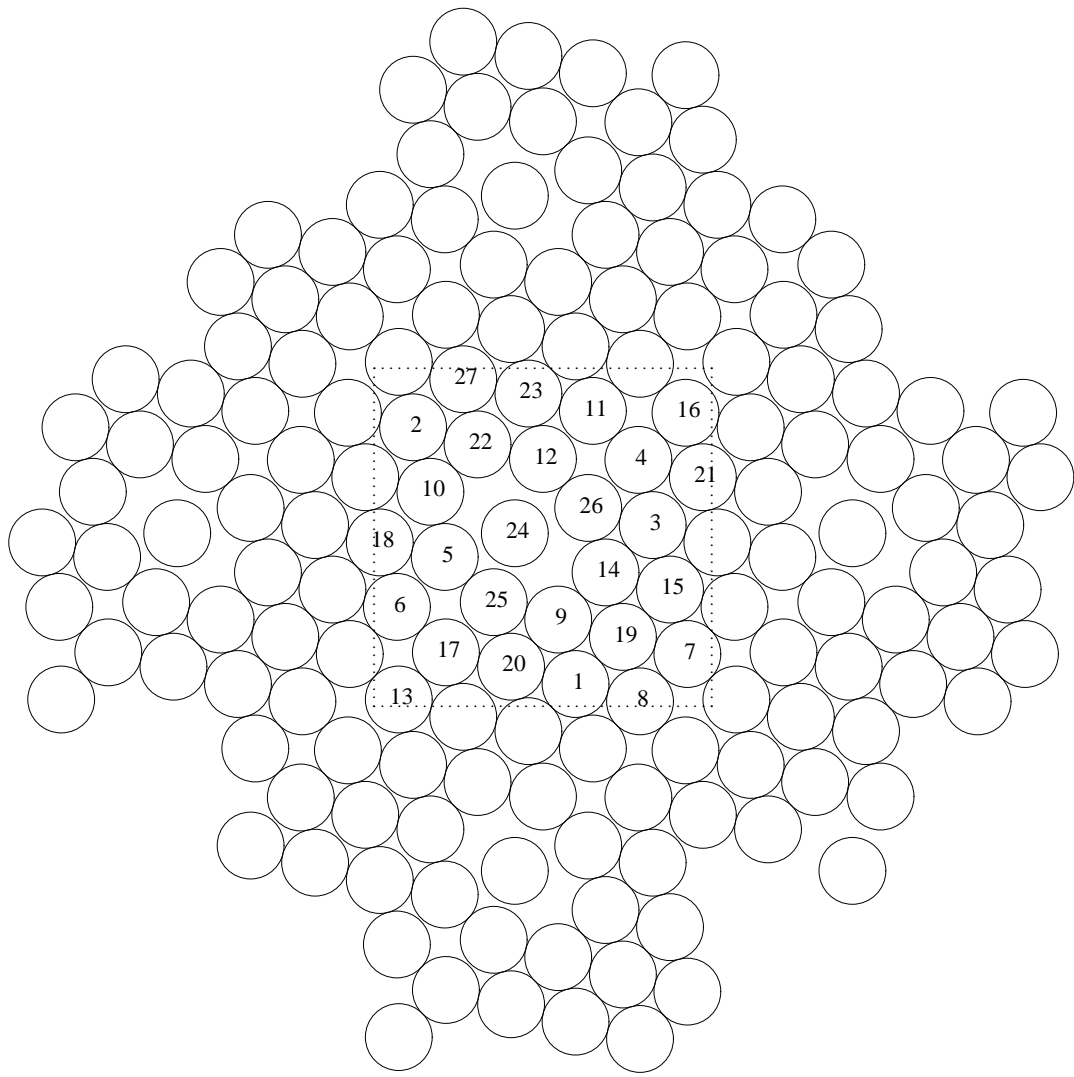


Figure 9.1: 27 disks after 100000 collisions; disk 24 is a rattler

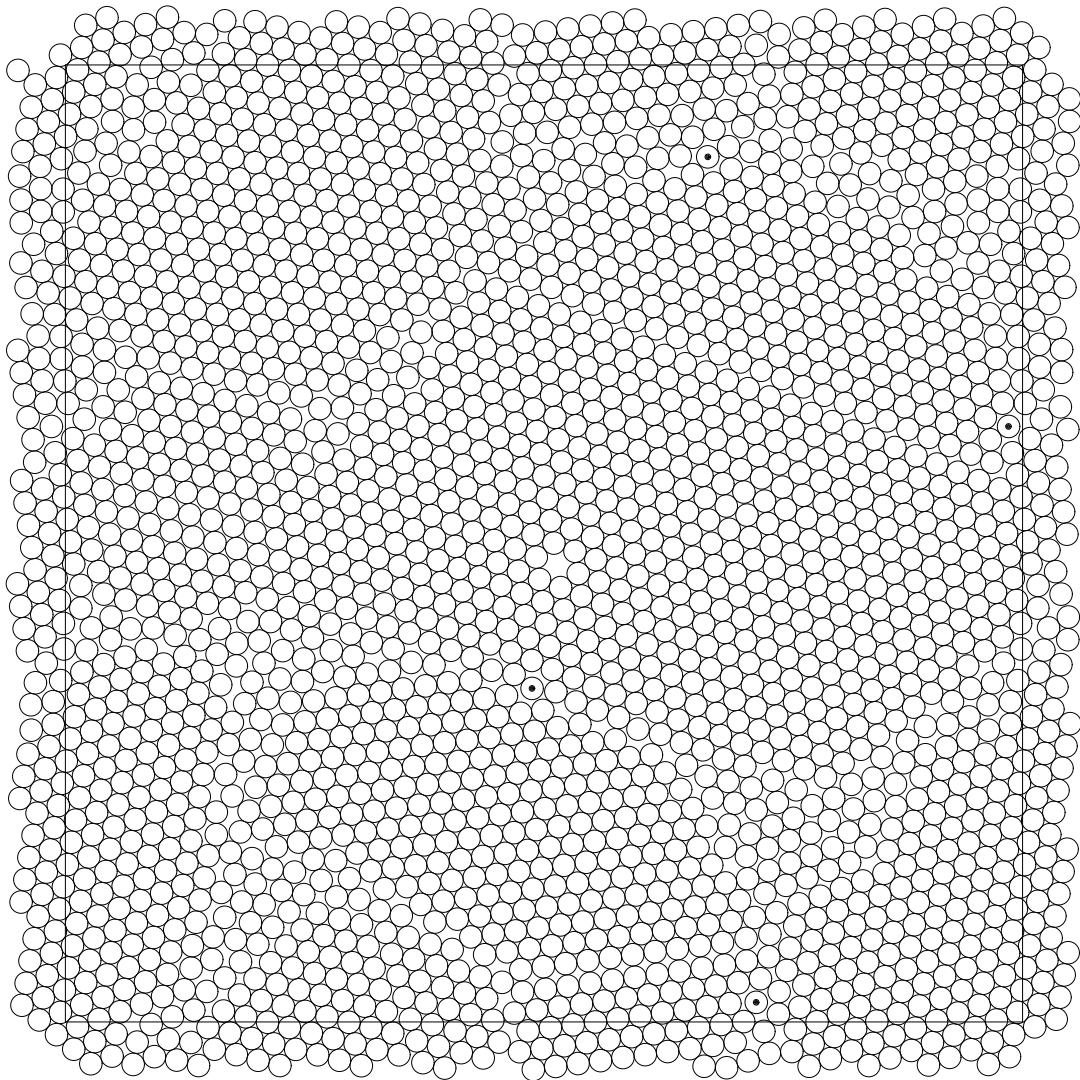


Figure 9.2: 2000 disks after 42×10^6 collisions. Dots mark significant rattlers

in [5]. The run was continued until the number reached 52000 as in [5]. It took 90 seconds CPU to complete this run.

A similar run in [5] (Series I) on one PE took 440 seconds and took 62 seconds on 32 nodes of a hypercube MARK III. (For 32 and 64 sectors, it took, respectively, 44 and 42 seconds in [5].) It is known [4] that one node of MARK III is about 60% faster than a VAX 8550, the host computer in [7]. Besides, algorithm [7] is a Fortran code while program [5] is written in the C-language, both compiled under *UNIX*TM. This yields an additional 10% in favor of algorithm [7], since Fortran is slower than C under a *UNIX*TM compilation.

Thus, one concludes that the serial algorithm [7] runs about as fast as the parallel Time Warp [5] on a 32-node hypercube. ¹

11. Other billiard-like simulations

A collision of two billiard balls of radius $D/2$ each can be considered as an interaction of two zero-size particle with potential $V(r) = 0$ for distances $r > D$ and $V(r) = +\infty$ for $r \leq D$. More general piece-wise constant potentials can be dealt with using the same algorithm, e.g., the square-well potential [1]:

$$\begin{aligned} V &= +\infty, & \text{if } r < \sigma_1 \\ V &= V_0, & \text{if } \sigma_1 < r < \sigma_2 \\ V &= 0, & \text{if } \sigma_2 < r \end{aligned} \tag{17}$$

where V_0 , σ_1 , and σ_2 are finite constants. We can imagine two concentric balls: the “hard core” ball of diameter σ_1 and a larger external ball of diameter σ_2 and correspondingly two types of “collisions”: internal, of the hard-cores and of the external balls. Each type has its own *jump* function.

By the Monte-Carlo simulation [9] shows that larger particles move against the gravitational force if placed in a vibrating container together with smaller particles. The balls of different diameters can be easily handled in our scheme, if the ball diameter becomes a part of its *state*. The model [9] can be easily simulated using direct representations of particle dynamics, rather than by Monte-Carlo.

The inhomogeneity of components, in general, can be treated in the same way, i.e., by making the type or the class identification of a component an unchangeable part of its *state*. Combat simulations [11] present such inhomogeneity to a large extend, since here a component represents a military unit of one of the two opposing armies and there are many types of such units.

Collisions may be generalized to any state changes, not necessarily immediately leading to the trajectory change. A typical simulation rule in [11] looks like follows: “if within

¹After the measuring run was completed, A.P. Wieland kindly informed the author that one sector boundary crossing is actually counted as two events in [5] rather than as one, as is assumed in this paper. Also, one pairwise disk collision is counted not as two events as assumed, but as $4+m$ events, where variable m is the number of disks located in the involved sectors at the time of the collision. Suppose only one sector is involved in each collision, and there are totally 16 sectors (as in Series I in [5]). Then m is about 10. This makes the total count of events generated in [5] during a comparable simulation time interval several times higher than was assumed in the experiments. This, in turn, makes program [7] faster than program [5].

radius σ , a unit detects m units of the same army and n units of the opposing army, then it takes course of action $c(n, m)$ from the time of detecting this situation until the time when another rule becomes applicable.” We can represent the set of these rules by surrounding a zero-sized unit by several circles, each representing one such a rule, A counter “inside” the unit state gets an instantaneous increment, when a particular circle “collides” with another unit. The counter change may or may not trigger the change of the course of the actions. Such mechanisms can be represented within the discussed framework and simulated using the algorithm in Figure 4.1.

According to [10], a variant of the dense packing algorithm can be used in finding optimal spherical codes. Here the task is to find N points $p_i, i = 1, \dots, N$, on the sphere in the k -dimensional Euclidean space in such a way that $\min_{i \neq j} \text{distance}(p_i, p_j) \rightarrow \max$. We would start with a random configuration of N points and then grow “caps” of equal size each cap having one point as the center. Caps are prevented from the overlap by the mean of collisions.

References

- [1] B.J. Alder and T.E. Wainwright, Studies in molecular dynamics. I. General method, *Journ. Chem. Phys.*, **31**, 2 (1959), 459–466.
- [2] C.J. Bashe et al., *IBM’s early computers*, MIT Press, 1986.
- [3] Erpenbeck, J.J., and Wood, W.W., Molecular dynamics techniques for hard-core systems, in *Statistical mechanics. Part B: Time-dependent processes*, Berne, J.B., ed., Plenum, New York, 1977, p.1–40.
- [4] Fox, G.C., The hypercube and the Caltech concurrent computation program: a microcosm of parallel computing, in *Special purpose computers*, Alder, B.J., ed., Acad.Press, New York, 1988, p.1–40.
- [5] P. Hontales, B. Beckman, et al., Performance of the colliding pucks simulation of the Time Warp operating systems, *Proc. 1989 SCS Multiconference, Simulation Series, SCS*, **21**, 2, p.3–7.
- [6] J. Katzenelson, Computational structure of the N-body problem, *Siam J. Sci. Stat. Comput.*, **10**, 4 (1989), p.787–815.
- [7] B.D. Lubachevsky and F.H. Stillinger, Geometric properties of random disk packings, *J. Statistical Physics*, **60**, 5/6, (Sept. 1990) p.561–583.
- [8] Lubachevsky, B.D., Simulating colliding rigid disks in parallel using bounded lag without Time Warp, *Proc. 1990 SCS Multiconference, Distributed Simulation, Simulation Series, SCS*, **22**, 1/2, p.194–202.
- [9] Rosato, A., et al., Why the Brazil nuts are on top: size segregation of particulate matter by shaking, *Physical Review Letters*, **58**, 10 (1087), p.1038–1040.

- [10] W. Smith, Private communication.
- [11] F. Wieland, and D. Jefferson, Case studies in serial and parallel simulation, *Proc. 1989 Int. Conf. Parallel Processing*, Vol.III, Ris, F. and Kogge, M., eds., p.255–258.